Modeling the Thermal Behavior of a Photoelectric-Thermal Device

Boysori Yuldoshov[1], Azamat Narbayev[1], Tulkin Buzrukov[2], Jasur Khaliyarov[1], Ural Berdiyev[1], Sirojiddin Toshpulatov[1] and Sojida Raupova[3]
[1]*Termez State University, Barkamol avlod Str. 43, Termez city, Uzbekistan*
[2]*Termiz University of Economics and Service, Farovon Str. 4B, Termez city, Uzbekistan*[2]
[3]*Termiz State Pedagogical Institute, At-Termiziy Str. 1A, Termez city, Uzbekistan*
b.yuldoshov10@mail.ru, narbaev@ro.ru, tolqinbuzrukov@gmail.com, xjxjasur@mail.ru, berdiyevu@tersu.uz, toshpulatovs@tersu.uz, sojidaraupova38@gmail.com.

Keywords: Photovoltaic Panel, Photothermal Device, Heat Collector, Solar Radiation, Temperature.

Abstract: This paper presents a numerical study of the thermal behavior of a photovoltaic-thermal (PVT) device using COMSOL Multiphysics. The research focuses on analyzing temperature distribution on the photovoltaic (PV) surface under varying solar radiation levels and coolant flow rates. A coupled model integrating laminar fluid flow and heat transfer in solids and fluids was developed to simulate the interaction between thermal and hydrodynamic processes within the system. Simulations were conducted for solar radiation intensities of 500, 700, 1000, and 1500 W/m², with corresponding water mass flow rates ranging from 0.0083 to 0.033 kg/s. The inlet water temperature was fixed at 15°C. The results demonstrate that increasing the coolant flow rate significantly reduces the PV surface temperature, thereby improving electrical efficiency, while higher solar radiation enhances thermal energy output. The study confirms that the integration of a heat collector and reflectors improves both thermal and electrical performance of the PVT system. A balance between radiation intensity and cooling conditions is essential to maintain PV operating temperatures within optimal limits. The modeling results are consistent with experimental observations, validating the effectiveness of the proposed approach for optimizing PVT system design.

1 INTRODUCTION

The installed solar power capacity in the world energy sector is increasing year by year and will exceed 1.4 TW in 2023, with China (609 GW) having the best performance. Renewable energy capacity is expected to increase to 473 GW (+13.9%) in 2023, with solar power accounting for 346 GW (+32.2%), followed by wind power with 116 GW (+12.9%) [1] (Figure 1).

The increasing efficiency of solar cells in converting solar energy into electricity is also driving the widespread use of this type of energy devices [2] (Figure 2).

Cooling PV (Photovoltaic Panel) panels, which convert solar energy directly into electricity, is considered effective in preventing the electrical efficiency from decreasing under the influence of high temperatures [3]-[7]. This cooling can consist of active, passive, or hybrid cooling systems [8]-[10]. A device equipped with such a cooling system is called a PVT (photovoltaic-thermal). The main purpose of such devices is to ensure that the PV electrical efficiency does not decrease due to temperature and to obtain additional thermal energy [11]-[15].

The part that extracts the heat is called the heat collector (HC). The more heat-conducting material that is attached to the PV surface, the more thermally and electrically efficient the device will be.

Modeling the physical processes occurring in PVT devices is also an important area [16]-[20]. Modeling is commonly used to analyze expected results without constructing an experimental device [21], [22]. In modeling, it is usually necessary to make some simplifications and specify initial conditions depending on the purpose [23]-[25].

Analytical formulations describing the energy balance and thermal characteristics of different components of PVT systems were reported in [26]. Several studies have also addressed the hydrodynamic behavior of PVT systems [27]-[28], alongside mathematical modeling approaches that

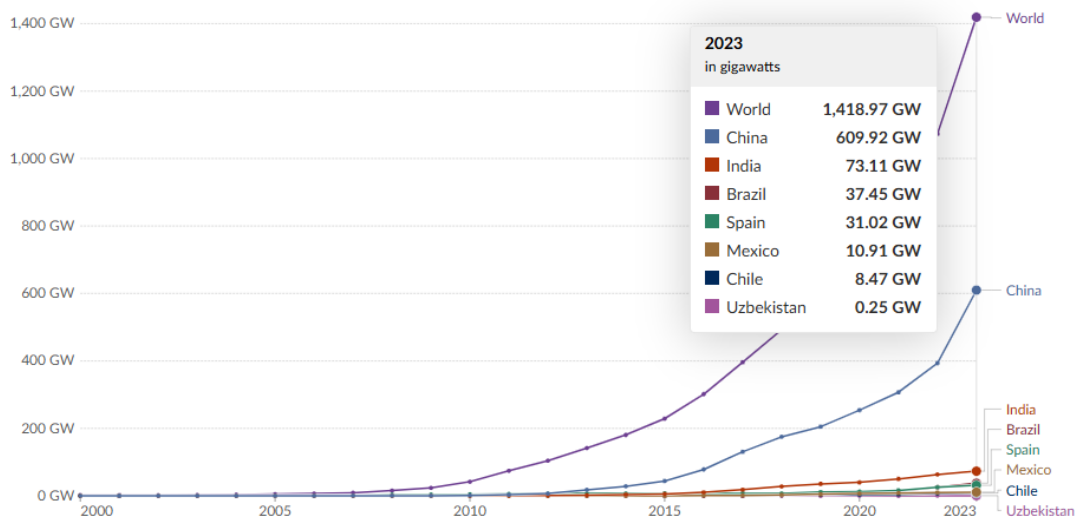

Figure 1: Installed solar energy capacity from 2000 to 2023

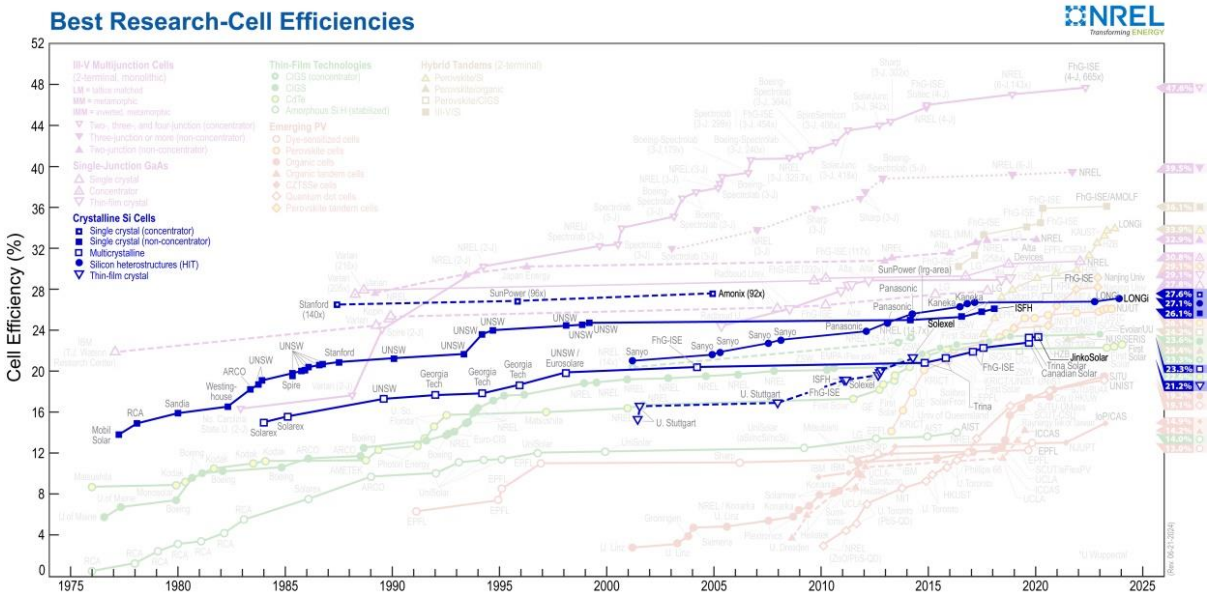

Figure 2: Crystalline silicon module efficiency

evaluate their electrical and thermal performance [29], [30]. Since solar energy represents a more sustainable option compared to other renewable sources, research in this field remains highly significant. This study focuses on analyzing the variation of thermal parameters in PVT systems through mathematical modeling.

Since we have already covered the practical part of our work in our previous work, let's focus only on the part based on the results obtained in the Comsole Multiphysics program.

2 METHODS AND MATERIALS

An overview of the main PVT device of the experiment is shown in Figure 3. The main function of reflectors is to increase the solar energy density and increase the thermal energy efficiency of the device. The water passing through the heat collector ensures that the PV panel temperature does not exceed the set point. These two aspects were taken into account in the modeling, and results were obtained for different values of solar radiation falling on the surface of the PV panel and water

mass flow. A monocrystalline silicon PV module with a maximum output power of 60 W was employed in the device. The specifications of the PV panel, along with the corresponding PVT system parameters derived from it, are summarized in Table 1.

Table 1: Geometric dimensions, physical and technical characteristics of PVT parts.

Parameters	Dimension
Geometric dimensions	
PV surface, S_{PV}	0.36m^2
PV frame width, d	2.5sm
Reflector surface, S_{ref}	0.36m^2
Reflector thickness, d_{ref}	0.4sm
The surface of the back cover, S_q	0.36m^2
The thickness of the back cover, d_q	0.4sm
Physical and technical characteristics	
Maximum power of PV, P_{max}	60W
Electrical efficiency of PV, η	16.5%
Open circuit voltage of PV, U_{oc}	24.4V
Short circuit current of PV, I_{sc}	3.33A
The fill factor of the PV's volt-ampere characteristic, FF	0.74
Reflection coefficient of the reflector, R	0.5
Water capacity of the heat collector,V	9 litre

The modeling studied the temperature distributions on the back surface of the panel, which are observed as a result of the effects of the heat collector and reflector of this device.

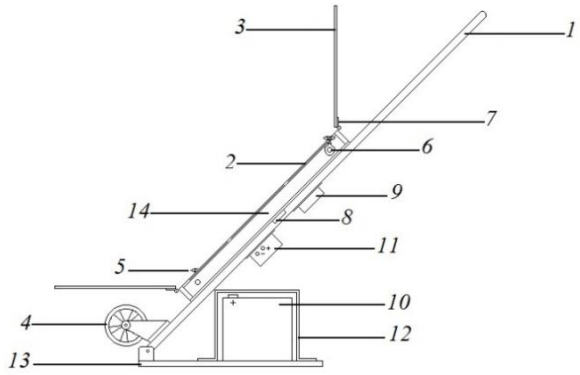

Figure 3: General view of the PVT device:

1 – structure handle, 2 – PV, 3 – reflectors, 4 – wheels of a small portable structure, 5, 6 – taps, 7 – hinges, 8 – positive and negative terminals of the electrical output of the PV, 9 – controller, 10 – battery, 11 – inverter, 12 – battery box, 13 – base of a small portable structure, 14 – heat collector.

The modeling was performed in the COMSOL Multiphysics 6.0 integrated software environment in the following sequence. After entering the program, the "Model Wizard" → "3D" sections were selected. To describe the heat exchange of water flow and the amount of heat absorbed in the PV with moving water in the HC, the "Laminar Flow (spf)" and "Heat Transfer in Solids and Fluids (ht)" interfaces were connected via the "Nonisothermal Flow" multiphysics interface. For the process under study, a new file with the extension ".mph" was created by selecting the "General Studies" → "Stationary" → "Done" sections.

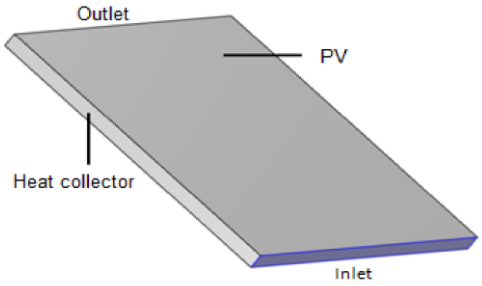

Figure 4: Part of PVT extracted for mathematical modelling.

The dimensions and parameters of the required geometric parts are selected through the "Model Builder" → "Component" → "Geometry" → "Block" sections, and the model geometry to be created through the "Build All Objects" section is displayed in 3D in the "Graphics" window. "The values of the variables and their units were described in the "Model Builder" → "Definition" → "Variables" sections. Through the "Definition" → "Selection" → "Explicit" sections, boundaries such as "Inlet", "Outlet", "Heat wall", and "Wall" were created and linked to variable values.

Using the "Model Builder" → "Materials" sections, "water" was selected from the material library as the cooling fluid. In this case, the values of all physical quantities for water are automatically loaded into the model.

Values such as "Inlet", "Outlet", "Wall" were created from the "Model Builder" → "Laminar Flow (spf)" section, and the lower part was selected for the "Inlet" section, considering that water moves from bottom to top. The water flow for the inlet section was expressed in kg/s. The upper boundary was selected for the "Outlet" section. The two sides and the back were defined as the boundary as thermal insulation and the front as the heat source passing through the back surface of the PV.

The energy density flux value for the heat source in W/m^2 is entered in the parameter-dependent state through the "Model Builder" → "Heat Transfer in Fluids" → "Heat Flux" sections. During the calculation of the results, the parameter values were changed, resulting in different results.

The "Model Builder" → "Multiphysics" → "Mesh" sections were selected, and the "Normal" section was selected for the "Element size". The model mesh part was created through the "Build All" section (Figure 5).

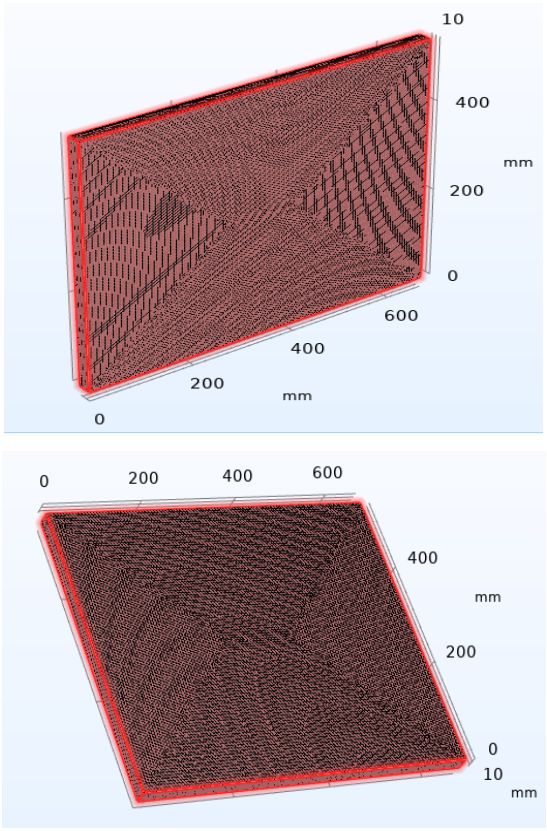

Figure 5: General condition of the mesh part

In the modeling process, the stationary Navier-Stokes equation was used in the blog through nonlocal connections and solved together with the continuity equation:

$$\rho(u\cdot\nabla)u = \nabla\cdot\left[-pI + K\right] + F \quad (1)$$

$$\rho\nabla\cdot u = 0 \quad (2)$$

Here ρ is the density of water (kg/m3), u is the flow velocity (m/s), I is the momentum (kg·m/s), K is the kinetic energy (J), and F is the external force (N).

The boundary conditions are set as follows:

- The fluid does not slip on the walls (boundaries) of the HC, i.e. u=0, the flow velocity is zero;
- The velocity of the liquid entering the HC is directed along the normal to the entrance surface;
- The pressure difference at the outlet from the HC is zero.

The "Heat Transfer in Fluids" interface was used for HC and PV heat transfer. The following heat balance equation for solids and heat transfer equations between layers were solved:

$$\rho c_p u\nabla T + \nabla q = \sum Q_i \quad (3)$$

$$q = -k\nabla T \quad (4)$$

where, u is the velocity of water (m/s), cp is the heat capacity (J/(kg°C)), q is the heat flux density (W/m^2), k is the heat transfer coefficient (W/(m^2°C))

3 RESULTS AND DISCUSSION

In the modeling, several suitable values of water consumption entering the cooling system, determined in the experiment, were entered and the results were obtained (Figure 6). It is estimated that 0.9 part of the total solar energy falling on the surface of the PV is completely absorbed, of which 0.75 part is spent on thermal energy, 0.15 part on electrical energy, and 10% on various heat and electrical losses. In this case, the portion of the 1500 W/m^2 solar radiation falling on the PV surface that is converted into thermal energy is equal to 1015 W/m^2, and in the calculations, the back surface of the PV was considered as a source of thermal energy. The initial temperature of the incoming water was taken as 15^{o}C (~288.15K). Figure 6 shows the results for water consumption values of a) 0.0083 (kg/s), b) 0.0167 (kg/s), c) 0.025 (kg/s), and d) 0.033 (kg/s). The HC boundary assumes a value of 1015 W/m^2 for the energy flux density as a heat source. The ambient temperature is assumed to be 15^{0}C (288.15K). From the graphs, the PV back surface temperature decreases as water consumption increases.

In the modeling, the water temperature at the back surface of the PV and the HC for different values of solar radiation incident on the PV surface, with the water consumption constant (0.01667 kg/s), is given in Figure 7.

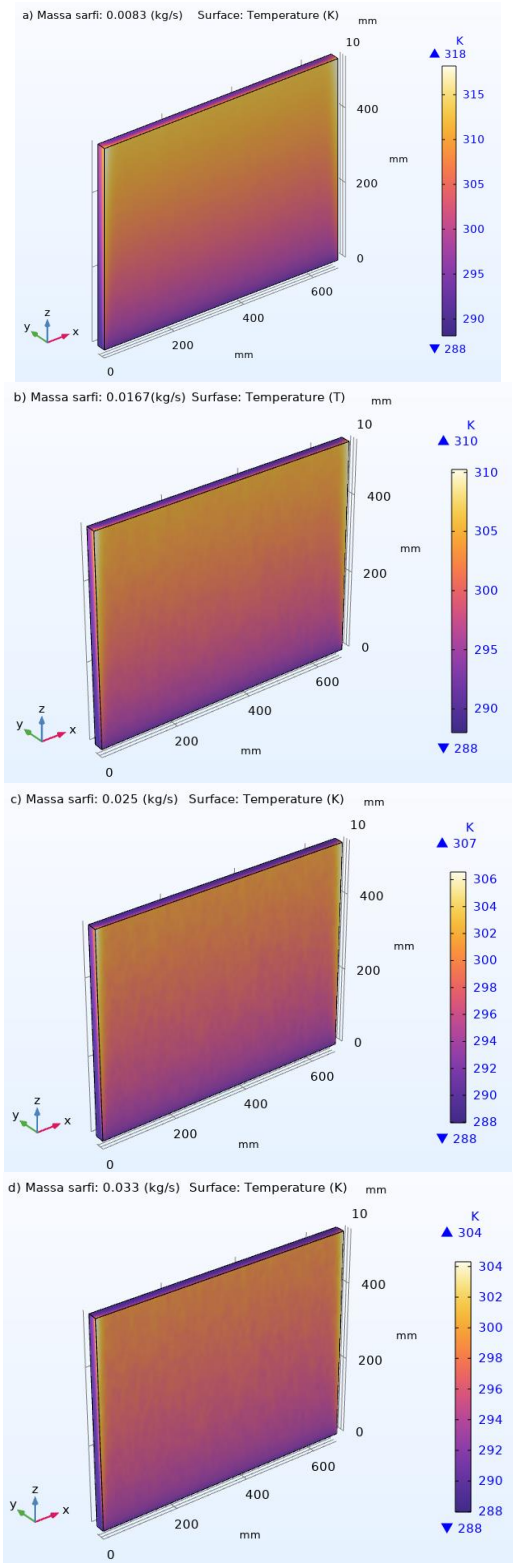

Figure 6. Temperature of the back surface of the PV at different values of water consumption entering the HC

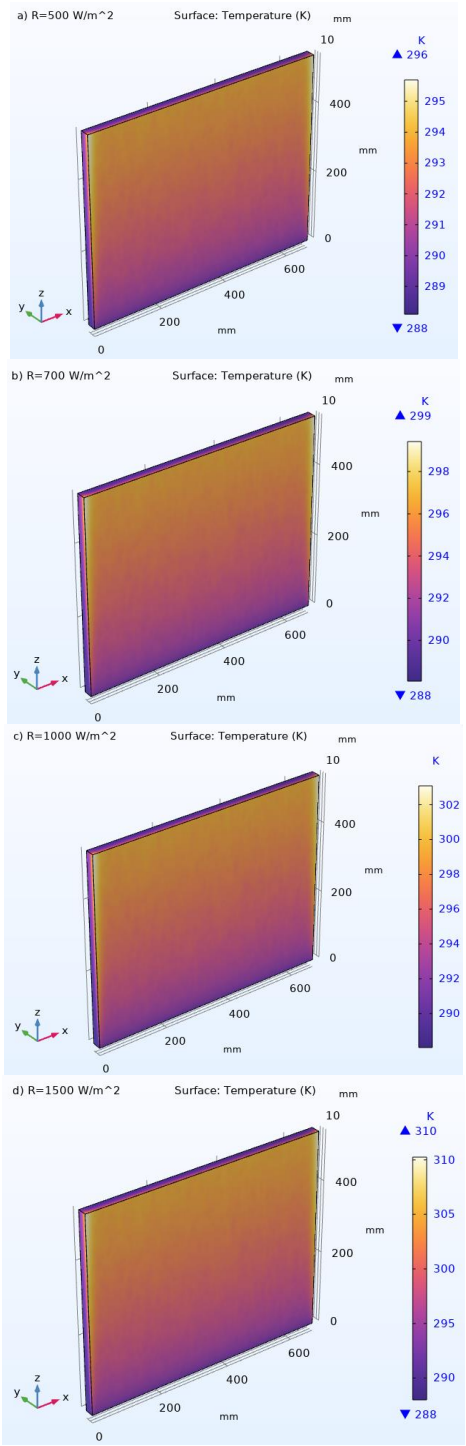

Figure 7: Surface temperature distribution at different values of radiation incident on the PV surface (water consumption (0.01667 kg/s)).

The results were obtained for the cases where the solar radiation incident on the PV surface was a) 500 W/m^2 b) 700 W/m^2 c) 1000 W/m^2 and

d) 1500 W/m^2. As solar radiation values increased, the PV back surface and outlet water temperatures increased steadily

Higher outlet water temperatures will inevitably lead to an increase in thermal energy. However, at the same time, this situation should not negatively affect the electrical parameters of the PV. The modeling results show that the maximum difference in PV rear surface temperatures was 37^{0}C (1500 W/m^2). The fact that the PV temperature is less than 60 ^{0}C is the basis for lower electrical losses due to its temperature.

At a simulated solar radiation value of 500 W/m^2, temperature differences are very small, with a value of 8^{0}C recorded. At these values, the efficiency of thermal energy utilization decreases sharply. For this purpose, it should be noted that reflectors serve as a key component for increasing the solar energy density. Increasing radiation increases the thermal efficiency of the system. However, increasing radiation values also requires consideration of PV temperature limits.

In the results obtained under natural conditions, the difference in water temperatures at the inlet and outlet was 5-30^{0}C. In this case, the water consumption and radiation values at the inlet were within the range of values used in the modeling. Therefore, the modeling and simulation results are consistent with the results obtained in real-world experiments.

4 CONCLUSIONS

The heat distribution on the PV surface and the temperature of the hot water that can be obtained from the heat collector are important. Through programming work performed in the Comsole multiphysics program, the heat distribution on the surface was studied at different values of radiation and water consumption. The graphs confirm that the temperature of the water leaving the HC reaches 30^{o}C with a maximum radiation of 1500W/m^2 and a water consumption of 0.0083kg/s. The modeling results show that at a water consumption of 0.017 kg/s, the temperature difference between the incoming and outgoing water is up to 20oC, and thus the temperatures on the PV surface are also maintained within this temperature range. This is the basis for improving electrical and thermal efficiencies by simultaneously increasing and cooling the incident radiation

REFERENCES

[1] IRENA, Renewable capacity statistics 2023. Abu Dhabi, UAE: International Renewable Energy Agency, 2023. [Online]. Available: https://www.irena.org/-/media/Files/IRENA/Agency/Publication/2023/Mar/IRENA_-RE_Capacity_Highlights_2023.pdf.

[2] National Renewable Energy Laboratory, “Solar cell efficiency.” [Online]. Available: https://www.nrel.gov/pv/cell-efficiency.html.

[3] M. Khamooshi, H. Salati, F. Egelioglu, A. H. Faghiri, J. Tarabishi, and S. Babadi, “A review of solar photovoltaic concentrators,” Int. J. Photoenergy, pp. 1–17, 2014.

[4] M. Tursunov et al., “Analysis of electric and thermal efficiency of crystal silicon small power suppliers,” Proc. Int. Conf. Applied Innovation in IT, vol. 11, no. 2, pp. 167–171, 2022, doi: 10.25673/113009.

[5] W. He, J. Zhou, C. Chen, and J. Ji, “Experimental study and performance analysis of a thermoelectric cooling and heating system driven by a photovoltaic/thermal system,” Energy Convers. Manag., vol. 84, pp. 41–49, 2014.

[6] A. Monjezi et al., “Development of an off-grid solar energy powered reverse osmosis desalination system with integrated photovoltaic thermal cooling,” Desalination, vol. 495, pp. 1–7, 2020.

[7] H. Nasef, S. Nada, and H. Hassan, “Integrative passive and active cooling system using PCM and nanofluid for thermal regulation of concentrated photovoltaic solar cells,” Energy Convers. Manag., vol. 199, pp. 1–15, 2019.

[8] U. Sajjad, M. Amer, H. Ali, A. Dahiya, and N. Abbas, “Cost effective cooling of photovoltaic modules to improve efficiency,” Case Stud. Therm. Eng., vol. 14, pp. 1–7, 2019.

[9] S. Bhakre, P. Sawarkar, and V. Kalamkar, “Performance evaluation of PV panel surfaces exposed to hydraulic cooling—A review,” Sol. Energy, vol. 224, pp. 1193–1209, 2021.

[10] B. Yuldoshov et al., “Analysis of electrical parameters of a metal collector photovoltaic-thermal device,” Proc. Int. Conf. Applied Innovation in IT, vol. 13, no. 1, pp. 243–247, doi: 10.25673/119239.

[11] M. Arefin, “Analysis of an integrated photovoltaic thermal system by top surface natural circulation of water,” Front. Energy Res., vol. 7, pp. 1–10, 2019.

[12] F. Sobhnamayan, F. Sarhaddi, M. Alavi, S. Farahat, and J. Yazdanpanahi, “Optimization of a solar photovoltaic thermal water collector based on exergy concept,” Renew. Energy, vol. 68, pp. 356–365, 2014.

[13] F. Yazdanifard, E. Ebrahimnia-Bajestan, and M. Ameri, “Investigating the performance of a water-based photovoltaic/thermal collector in laminar and turbulent flow regime,” Renew. Energy, vol. 99, pp. 295–306, 2016.

[14] Z. Ul Abdin and A. Rachid, “Bond graph modeling of a water-based photovoltaic thermal collector,” Sol. Energy, vol. 220, pp. 571–577, 2021.

[15] S. Prasetyo, A. Prabowo, and Z. Arifin, “The use of a hybrid photovoltaic/thermal collector system as a sustainable energy-harvest instrument in urban technology,” Heliyon, vol. 9, 2023.

[16] D. Luca et al., “Modeling of energy and exergy efficiencies in high vacuum flat plate photovoltaic–thermal collectors,” Energy Rep., vol. 9, pp. 1044–1055, 2023.

[17] E. Touti et al., “Experimental and numerical study of the PVT design impact on electrical and thermal performances,” Case Stud. Therm. Eng., vol. 43, pp. 1027–1032, 2023.

[18] M. Attia et al., “Thermal analysis on the performance of a finned hybrid bi-fluid PVT system,” Therm. Sci. Eng. Prog., vol. 45, pp. 1021–1035, 2023.

[19] P. Bradshaw, “Turbulent secondary flows,” Annu. Rev. Fluid Mech., pp. 53–74, 1987.

[20] B. Yuldoshov et al., “Mathematical modeling of heat parameters of photothermal device,” Proc. Int. Conf. Applied Innovation in IT, vol. 12, no. 2, pp. 131–137, doi: 10.25673/118125.

[21] S. Ferrari, L. G. Paterna, and A. Romano, “A review of laboratory and numerical techniques to study turbulence and flow structures,” J. Hydraul. Res., vol. 56, no. 1, pp. 1–19, 2018, doi: 10.1080/00221686.2017.1375454.

[22] K. Degeling, R. Baxter, and J. W. Crommelin, “Introduction to metamodeling for reducing computational cost in simulation-based analyses,” Reliab. Eng. Syst. Saf., vol. 187, pp. 97–109, 2019, doi: 10.1016/j.ress.2019.03.004.

[23] T. Sun et al., “Modeling and simulation analysis of photovoltaic photothermal modules in solar heat pump systems,” Energies, vol. 17, no. 5, art. 1042, 2024, doi: 10.3390/en17051042.

[24] L. Ma, Z. Wang, D. Lei, and L. Xu, “Establishment, validation, and application of a comprehensive thermal hydraulic model for a parabolic trough solar field,” Energies, vol. 12, no. 16, art. 3161, 2019, doi: 10.3390/en12163161.

[25] S. K. Shoguchkarov et al., “Verification of a mathematical model for a photovoltaic thermal-thermoelectric generator unit,” Appl. Sol. Energy, vol. 57, pp. 384–390, 2021, doi: 10.3103/S0003701X21050121.

[26] S. Diwania et al., “Modeling and assessment of the thermo-electrical performance of a photovoltaic-thermal system using nanofluids,” J. Braz. Soc. Mech. Sci. Eng., vol. 43, art. 190, 2021, doi: 10.1007/s40430-021-02909-6.

[27] I. Guarracino, A. Mellor, N. J. Ekins-Daukes, and C. N. Markides, “Dynamic coupled thermal and electrical modelling of hybrid photovoltaic/thermal collectors,” Appl. Therm. Eng., vol. 101, pp. 778–795, 2016, doi: 10.1016/j.applthermaleng.2016.02.056.

[28] A. Shahsavar and M. Ameri, “Experimental investigation and modeling of a direct-coupled PV/T air collector,” Sol. Energy, vol. 84, no. 11, pp. 1938–1958, 2010, doi: 10.1016/j.solener.2010.07.010.

[29] Z. Wang et al., “Numerical investigation of innovative photovoltaic–thermal collector designs,” Energies, vol. 17, no. 10, art. 2429, 2024, doi: 10.3390/en17102429.

[30] A. M. Soliman, “A numerical investigation of PVT system performance with various cooling configurations,” Energies, vol. 16, no. 7, art. 3052, 2023, doi: 10.3390/en16073052.